

Sensor Networks With Mobile Access: Energy and Capacity Considerations

Gökhan Mergen, *Member, IEEE*, Qing Zhao, *Member, IEEE*, and Lang Tong, *Fellow, IEEE*

Abstract—Sensor network with mobile access (SENMA) is an architecture in which randomly deployed low-power sensors are orchestrated by a few powerful mobile access points (APs). This paper considers SENMA from energy-efficiency and information-theoretic perspectives. By allowing sensors to propagate data directly to mobile APs over multiaccess channels, and relieving sensors from energy-consuming network functions, SENMA has the potential of offering orders of magnitude of improvement in energy efficiency over the multihop ad hoc architecture, as demonstrated by our analysis on scalability. Optimization configurations of SENMA such as the altitude, the trajectory, and the coverage of APs are considered next, using the sum-rate as the performance metric. Optimal strategies for single and multiple APs are determined. For multiple APs, the possibility of and the gain due to cooperation (i.e., joint decoding of signals received at different APs) are investigated.

Index Terms—Capacity, energy efficiency, mobile access points (APs), multiple access, sensor networks.

I. INTRODUCTION

WE CONSIDER sensor network with mobile access (SENMA)—an architecture for low-power and large-scale sensor networks [1] (see Fig. 1). SENMA has two types of nodes: sensors and mobile access points (APs). Sensors, often deployed randomly in large quantity, are low-cost nodes with limited processing and communication capability. For some applications, such as radio frequency (RF) tags, sensors may even be passive. The primary function of sensors includes data collection, local processing, and data delivery to mobile APs. The mobile APs, in contrast, are powerful nodes, both in their communication and processing capability and in their ability to traverse the network. Examples are manned/unmanned aerial vehicles, ground vehicles equipped with power generators, or specially designed light nodes that can hop around in the

Paper approved by S. N. Batalama, the Editor for Spread Spectrum and Estimation of the IEEE Communications Society. Manuscript received May 4, 2004; revised June 15, 2005 and December 12, 2005. This work was supported in part by the Multidisciplinary University Research Initiative (MURI) under the Office of Naval Research Contract N00014-00-1-0564, in part by the Army Research Laboratory CTA on Communication and Networks under Grant DAAD19-01-2-0011, and in part by the Army Research Office under Grant ARO-DAAB19-00-1-0507. This paper was presented in part at the IEEE Military Communications Conference, Boston, MA, October 2003, and in part at the Allerton Conference on Communication, Control, and Computing, Monticello, IL, October 2003.

G. Mergen was with the School of Electrical and Computer Engineering, Cornell University, Ithaca, NY 14853 USA. He is now with Qualcomm, Inc., Campbell, CA 95008 USA (e-mail: gmergen@qualcomm.com).

Q. Zhao is with the Department of Electrical and Computer Engineering, University of California, Davis, CA 95616 USA (e-mail: qzhao@ece.ucdavis.edu).

L. Tong is with the School of Electrical and Computer Engineering, Cornell University, Ithaca, NY 14853 USA (e-mail: ltong@ece.cornell.edu).

Digital Object Identifier 10.1109/TCOMM.2006.884845

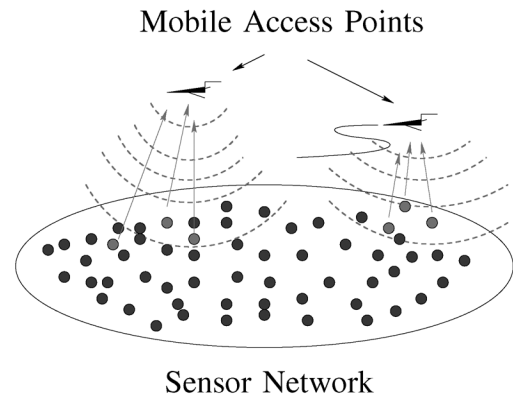


Fig. 1. Sensor networks with mobile access.

network. Mobile APs retrieve the data from sensors and deliver it to a remote control center (possibly via a satellite link). They need not always be present or operational along with the sensors; they may be called upon for data collection, or they may be embedded in the network, staying passive until called.

One can view SENMA as an “inversion” of the cellular architecture: mobile users in cellular networks correspond to stationary sensors in SENMA, stationary base stations, the mobile APs. In both architectures, the network has two types of nodes with a smaller number of powerful nodes taking the responsibility of network operations. Such a division of network function is crucial to the scalability with respect to the number of low-cost energy-constrained nodes: phones in the cellular network and sensors in SENMA.

There are several practical advantages of SENMA. At the physical layer, synchronization among sensors under the multihop ad hoc architecture can be difficult. In SENMA, however, sensors are driven by mobile APs; the presence of a strong beacon from the mobile AP significantly simplifies timing recovery and synchronization. For some applications, sensors need to know their locations. This, too, can be facilitated by the mobile APs. Different from the transmissions between low-lying antennas in ad hoc sensor networks where signal decays as the fourth power of distance [2], [3], the propagation channels in SENMA are likely to be line-of-sight, although sensors may need to transmit over a longer distance to reach the mobile APs. The medium-access control (MAC) layer of SENMA is also simplified; MAC becomes a many-to-one communication problem, allowing the use of a number of energy-efficient distributed schemes [4]–[6]. In SENMA, routing packets from one part of the network to another, if needed, can be carried out by mobile APs, relieving sensors from this energy-consuming task.

A. Summary of Results and Organization

The defining feature of SENMA is the addition of mobile APs to which sensors may communicate directly. We first focus on the benefit of such direct transmissions in terms of energy consumption. Our analysis in Section II takes into account energy spent in both transmission and listening. While the importance of the latter has been widely recognized, we show that in the absence of a perfect wake-up scheme, the cost of listening can be a dominant factor in a dense network. Specifically, we show that for a multihop ad hoc network with N sensors and under ideal MAC, routing, and hardware conditions, the energy consumed in retrieving one packet scales with either $\sqrt{N \log N}$ (when N is increased by increasing the node density) or $\sqrt{N(\log N)^{\alpha-1}}$ (when N is increased by increasing the network geographic size) where α is the path-loss factor. For SENMA, on the other hand, by relieving sensors from the energy-consuming tasks of multihop routing, the energy consumed by sensors depends on the channel propagation characteristics, but not the size of the network.

We consider next the design of SENMA with aerial APs in Section III. Specifically, we examine the effect of the altitude, the trajectory, and the coverage area of mobile APs on the sum-rate of the information retrieval. We consider the capacity of SENMA following the methodology of Shamai and Wyner [7], [8], who analyzed the information-theoretic capacity of multiaccess systems. Our objective, however, is not to find the capacity; we aim to gain insights into alternatives and tradeoffs in the design of SENMA. For example, we examine the tradeoff between increasing the altitude to improve sum-rate (by allowing more sensors to access the channel) and decreasing the altitude to save power. The optimal altitude is such that there are approximately 3~5 sensors within the coverage of the mobile AP. In Section III-B, we also consider the effect of sensor density on network capacity.

In a network with multiple APs, if the APs operate independently, then signals directed to different APs affect each other as interference. APs flying apart avoids interference and maximizes capacity. When multiple APs perform cooperative decoding (joint decoding on the fly or at the control center), the APs can mimic a receiver with multiple antennas. We show that, surprisingly, the optimal strategy with cooperation is to fly together as a group at low signal-to-noise ratio (SNR) and fly separately at high SNR. Furthermore, we show that cooperation among multiple APs does not improve the capacity in the high-SNR regime. Details and relative performances of these strategies are provided in Section III-D.

We discuss the capacity versus delay tradeoffs encountered in SENMA in Section IV.

B. Related Work

The SENMA architecture is first proposed in [1]. The MAC in SENMA was considered in [4]–[6], [9], and [10]. Most of the literature on sensor networks focuses on the flat multihop ad hoc architecture (see [11] for a survey). In [12], an extension of the multihop architecture with mobile sensors is considered, and a specific MAC protocol, Eavesdrop-And-Register, is introduced that integrates mobile nodes into the network. Nonetheless, the primary network functions in [12] are not handled by

the mobile nodes. In [13], the idea of using mobile nodes for message ferrying is considered, where the objective is to use mobiles to provide nonrandom proactive routes. Bansal and Liu considered the addition of mobile nodes to relay packets [14]. In [15], unmanned aerial vehicles (UAVs) are used to deploy sensors and serve as communication hubs. The settings considered in [15] are different from this paper. It is assumed that the distance among sensors is large, and a UAV is required to visit each sensor one at a time. An adaptive path-planning algorithm is proposed in [15] that finds the minimum-cost path for a UAV to visit every sensor. It has also been considered to introduce UAVs to sensor networks to serve as actuators [16] or mobile sensors [17] for target detection and tracking.

The energy-efficiency comparison between SENMA and the ad hoc architecture is first presented in [1], although the calculation there does not take into account the possibility of scaling the transmission radius according to the size of the network. The difference between previous analyses on energy consumption [18]–[20] and ours is that we explicitly account for energy consumed in both transmission and reception. The physical basis of our model comes from [21], where energy consumption is characterized at the circuit level. It is shown that the transceiver circuitry consumes two to three times more power in receiving than in transmitting.

The capacity analysis of a reachback channel [22], [23] is also applicable to SENMA, where the authors consider general correlated sources but restrict themselves to noninterfering sensors. Our capacity analysis does not include source correlation, but we explicitly consider the physical-layer aspects of SENMA, and other AP-related parameters that affect the network performance.

II. ENERGY-EFFICIENCY ANALYSIS

In this section, we study energy efficiency of SENMA as compared with the flat ad hoc (multihop) architecture. Based on an idealized network model, we aim to gain insights into the scaling behavior of the total energy expenditure of these two architectures.

A. The Network Model

Assume that N sensors are randomly and uniformly deployed on a disk of radius R . The node density ρ is given by $N/\pi R^2$. We analyze here the energy cost of moving one packet originated at a randomly chosen sensor to a gateway node located at the center of the sensor field (in flat ad hoc) or a mobile AP flying d meters above (in SENMA). For the flat ad hoc architecture, we assume sensors are capable of adjusting the transmission power to cover a neighborhood of radius r [see Fig. 2(a)]. In SENMA, we assume that the mobile AP can position itself at specific locations and activates sensors in its coverage area of radius $d \tan \theta$ where θ is adjustable [see Fig. 2(b)].

We assume perfect MAC for both architectures, i.e., every transmission is successful. It should be clear that MAC is much more difficult to handle under the flat ad hoc architecture than in SENMA, and is likely to result in a more significant overhead in energy consumption. For the flat ad hoc architecture, we assume that a minimum-energy route between the chosen sensor and the gateway node has been established at no cost.

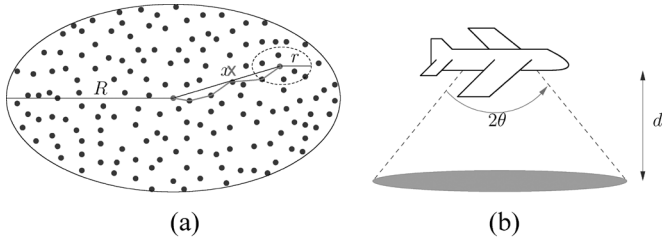


Fig. 2. (a) Flat ad-hoc network. (b) Mobile AP.

B. Radio Model and Wake-Up Scheme

When there is no on-going transmission, sensors are in the sleep state by turning off most of their transceiver circuits. A wake-up scheme is thus required to bring nodes to the active communication state when necessary. One approach is to wake up nodes by the RF signals, which can be achieved by equipping each node with an energy detector. Specifically, for the flat ad hoc architecture, a sensor is woken up by the transmission of its neighboring nodes. In this case, sensors cannot be woken up individually; every node within the range r of the transmitting node will be woken up and checked whether it is the intended receiver. In SENMA, sensors are woken up by the beacon signal from the mobile AP. (We assume that sensors are woken up by the beacon from the mobile AP, but not the transmission of other sensors. This can be achieved by, for example, using a different frequency band for the beacon signal. We realize that this may potentially complicate the receiver circuitry of the sensor nodes.) All sensors in the coverage area of the mobile AP are activated.

Another wake-up scheme assumes that each sensor w.p. p wakes up independently to detect whether there is any on-going transmission. The energy analysis is similar in this case by considering a network with pN nodes on the average.

A perfect wake-up scheme would be one that completely eliminates unnecessary energy consumption in overhearing, by bringing only the intended receiver back to the active state at exactly the time of transmission. One possible approach to a perfect wake-up scheme is to implement a global schedule; nodes are woken up by their internal clocks when scheduled for transmission or reception. For a large-scale sensor network with time-varying topology,¹ it is perhaps unrealistic to assume such a perfect global schedule can be established and maintained without introducing a significant amount of overhead. In this paper, we assume sensors are woken up by the RF signals detected by energy detectors. In the analysis, we ignore the energy consumed in sleeping; its inclusion is straightforward.

We use the radio model considered in [21] and [24]. When a node is receiving, it consumes E_{tx} Joule/bit; a transmission that covers a neighborhood of radius r consumes $E_{tx}(r)$ Joule/bit, which is given by [21]

$$E_{tx}(r) = e_{tx} + \max\{e_{min}, e_{out}r^\alpha\} \tag{1}$$

where α is the path attenuation factor, e_{tx} the energy consumed by the transmitter circuitry, e_{out} the antenna output energy to reach, with an acceptable SNR, the destination-unit distance

¹Sensors may become nonfunctional due to battery depletion or other environmental factors.

away, and e_{min} the minimum energy radiated regardless of the transmission range. Note that e_{min} imposes a hard limit on the minimum transmission range

$$r \geq r_0 \triangleq \left(\frac{e_{min}}{e_{out}} \right)^{\frac{1}{\alpha}}. \tag{2}$$

C. Energy Efficiency of Multihop Ad Hoc Sensor Networks

We now calculate, under a multihop ad hoc architecture, the total energy consumed by sensor nodes for moving one packet from a randomly chosen sensor to the gateway node located at the center of the network. As illustrated in Fig. 2(a), a chosen sensor broadcasts the packet, using a transmission range r , to its neighbors, and the one specified by the minimum-energy route will relay the packet toward the gateway node.

Let X denote the distance from the chosen sensor to the gateway node. The probability density function (pdf) of X is given by

$$p_X(x) = \frac{2}{R^2}x, \quad 0 < x \leq R. \tag{3}$$

The total energy $\mathcal{E}_{AdHoc}(r)$ consumed by moving one packet to the gateway node with an optimal transmission range r is given by

$$\mathcal{E}_{AdHoc} = \min_{r \geq r_{min}} \frac{2}{R^2} \int_0^R E(r)h(x,r)x dx \tag{4}$$

where r_{min} is the minimum transmission range to ensure network connectivity under the hardware constraint, $E(r)$ and $h(x,r)$ are, respectively, the energy consumed in one hop and the number of hops for a packet to reach the gateway node x meters away.

From [25], we know that a necessary and sufficient condition for network connectivity for large N is $r^2/R^2 = \mathcal{O}(\log N/N)$. We thus have, together from (2)

$$r_{min} = \max \left\{ r_0, R\sqrt{\frac{\log N}{N}} \right\}. \tag{5}$$

With a transmission range of r , a sensor has, on the average, $(N-1)(r^2/R^2)$ neighbors who listen to that sensor's transmission. We thus have²

$$E(r) = E_{tx}(r) + (N-1)\frac{r^2}{R^2}E_{tx}. \tag{6}$$

For simplicity, we assume that the transmitted packet contains one bit. A lower bound³ on the number $h(x,r)$ of hops is given by

$$h(x,r) \geq \left\lceil \frac{x}{r} \right\rceil. \tag{7}$$

It is shown in [26] that for $r \geq r_{min}$, this lower bound is achieved with probability (w.p.) 1, when N approaches infinity,

²Energy consumed in overhearing may not be the same as in receiving. For ease of presentation, we ignore this difference in the analysis. It is, however, straightforward to incorporate this difference. Obviously, it does not affect the scaling law.

³A tighter lower bound was given in [1]. The analysis there, however, is an approximation for $x \gg r$ and a dense network with sensors independently waking up.

by increasing either ρ or R . From (4)–(7), we have, w.p. 1, as $N \rightarrow \infty$

$$\begin{aligned} \mathcal{E}_{\text{AdHoc}} &= \min_{r \geq r_{\min}} \frac{2R}{3r} \left(E_{\text{tx}}(r) + (N-1) \frac{r^2}{R^2} E_{\text{rx}} \right) \\ &= \begin{cases} \mathcal{O}(\sqrt{N \log N}), & \rho \uparrow, r_0 = 0 \\ \mathcal{O}(N), & \rho \uparrow, r_0 > 0 \\ \mathcal{O}(\sqrt{N(\log N)^{\alpha-1}}), & R \uparrow. \end{cases} \quad (8) \end{aligned}$$

In all cases, the optimal transmission range in the asymptotic regime ($N \rightarrow \infty$) is given by r_{\min} , defined in (5). When the network size N is increased by increasing ρ , the energy consumed in listening dominates. When N is increased by increasing R , the dominating factor is the transmission energy. We point out that when the network size N is relatively small, or a perfect wake-up scheme is employed, the optimal transmission range may not be given by the minimum value r_{\min} . Comprehensive studies on the tradeoff between long-hop and short-hop routing can be found in [27]–[30] and references therein.

D. Energy Efficiency of SENMA

In SENMA, the mobile AP positions itself at a random location and broadcasts a beacon to activate sensors in its coverage area. One activated sensor then transmits directly to the mobile AP d meters away. Let θ_0 denote the minimum angle of the coverage area [see Fig. 2(b)]. The total energy consumed by sensors in this process is given by

$$\begin{aligned} \mathcal{E}_{\text{SENMA}} &= \min_{\theta \geq \theta_0} \frac{d^2 \tan^2 \theta}{R^2} N E_{\text{rx}} + E_{\text{tx}}(d) \\ &= \begin{cases} \mathcal{O}(1), & \rho \uparrow, \theta_0 = 0 \\ \mathcal{O}(N), & \rho \uparrow, \theta_0 > 0 \\ \mathcal{O}(1), & R \uparrow \end{cases} \quad (9) \end{aligned}$$

where the first term accounts for the listening energy consumed by all the sensors in the coverage area. Comparing (9) with (8), we see that when the network size N is increased by increasing R , SENMA offers orders of magnitude of improvement over the flat ad hoc architecture in energy efficiency. In a dense network ($\rho \uparrow$), SENMA is more energy-efficient when the hardware constraint θ_0 on the minimum coverage area is negligible. Shown in Fig. 3 is a numerical result on the ratio of the aggregated energy expenditure of flat ad hoc to that of SENMA as a function of the node density ρ . Typical transceiver power consumption values given in [21] are used. We see that when the hardware constraints on r (for flat ad hoc) and θ (for SENMA) are negligible, SENMA offers significant improvement which increases with the size of the network. When the hardware constraints are significant, the improvement achieved by SENMA levels off when ρ increases, due to the identical scaling behavior of these two architectures.

A few caveats are necessary to put the comparison between the two architectures in perspective. In the energy analysis, we focus on the energy consumption of the battery-powered sensor nodes. The energy consumed by the mobile AP and the gateway node is not included. The energy consumed by the mobile AP can be significantly larger than that of the gateway node, especially in networks deployed over a large area. Compared with sensor nodes, however, the mobile APs are far less energy-constrained, and can be easily recharged. The basic idea of SENMA

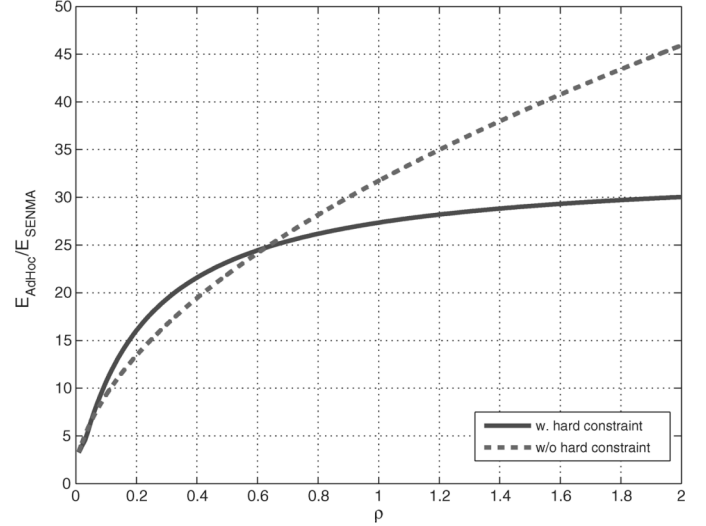


Fig. 3. Energy-efficiency comparison ($R = 500$ m, $d = 50$ m, $\alpha = 3$, $e_{\text{tx}} = 81$ nJ, $e_{\text{rx}} = 180$ nJ, $e_{\text{out}} = 0.1$ nJ, $r_0 = 10$ m, $d \tan \theta_0 = 10$ m).

is to relieve the resource-constrained sensors from energy-consuming tasks such as routing by exploiting the mobility of a few powerful APs.

We realize that the gain in energy efficiency achieved by SENMA may come at a price of a longer delay in data collection, as compared with the flat ad hoc architecture. Each architecture may have its own domain of applications. A delay analysis can put the comparison of these two architectures in a fuller context, which we will focus on in the future.

III. CAPACITY ANALYSIS

SENMA brings in some unique design issues that are not encountered under the multihop ad hoc architecture. For example, the position and trajectory of an aerial AP need to be controlled for optimal network operation. Another design issue is concerned with the interaction among multiple APs. In this section, we address these problems and study the capacity of SENMA (i.e., the maximum retrieval rate) from an information-theoretic perspective.

A. Problem Setup

In the analysis, it is assumed that the AP flies at an altitude d , and it can receive packets from angle 2θ [Fig. 2(b)]. The angle and altitude determines the coverage area of AP, which is a circle with radius $d \tan \theta$ and area $A := \pi d^2 \tan^2 \theta$. The AP continuously transmits a beacon to inform about its location. The sensors within the coverage area hear the beacon, wake up and send their data; the nodes outside the coverage stay in the sleep mode.

Consider a sensor network with N sensors. We use a discrete-time block-fading model to represent the received signal at the AP

$$\mathbf{y}(t) = \sum_{i \in \mathcal{J}(t)} h_i(t) \mathbf{x}_i(t) + \mathbf{n}(t) \quad (10)$$

where t is the block index (a block is a time unit of T symbols), $\mathcal{J}(t) \subset \{1, \dots, N\}$ is the set of nodes within the coverage in block t , $h_i(t) \in \mathbb{R}$ is the channel gain from sensor i to the AP, and $\mathbf{x}_i(t) \in \mathbb{R}^T$ the transmitted vector from sensor

i. In the block-fading model, the basic assumption is that the channel gain $h_i(t)$ and the coverage set $\mathcal{J}(t)$ stays constant during the block, and can change value between blocks. The noise $\mathbf{n}(t) \in \mathbb{R}^T$ is white Gaussian with variance σ^2 (i.e., $\mathcal{N}(0, \sigma^2 \mathbf{I})$), and is independent and identically distributed (i.i.d.) in time. The sensors have a short-term average power constraint P , i.e., $(1/T) \sum_{i=1}^T \mathbf{x}_i^2(t) \leq P$ for every i, t .

We assume that the AP coverage $\mathcal{J}(t)$ is a stationary (or periodic) process. In SENMA, the channel gains $h_i(t)$ are determined by the location of the mobile AP and the physical environment. For simplicity, we suppose that $\{h_i(t), t \geq 1\}$ form a stochastic process, i.i.d. for different t, i , and independent from $\mathcal{J}(t)$.⁴ The sum-capacity of the system is given by

$$C = \frac{1}{2} \mathbb{E}_{\mathbf{h}, \mathcal{J}} \log \left(1 + \frac{P \sum_{i \in \mathcal{J}} h_i^2}{\sigma^2} \right) \quad (11)$$

(proof follows directly from similar arguments in [7]).⁵ To achieve this rate, it is assumed that the channel side information $h_i(t)$ is known at the mobile AP, but not at the sensors. Since h_i 's are i.i.d. and independent from $\mathcal{J}(t)$, (11) can be simplified to

$$C = \frac{1}{2} \mathbb{E}_K \mathbb{E}_{\mathbf{h}} \log \left(1 + \frac{P \sum_{i=1}^K h_i^2}{\sigma^2} \right) \quad (12)$$

where K is the random variable denoting the number of elements in \mathcal{J} .

B. SENMA With Single Mobile AP

We will first focus on the problem of optimal coverage area for the mobile AP. Let the sensor density be ρ sensor/m². In general, the number of sensors in the coverage K is a random number. In the analysis, however, we will first consider the case that this number is deterministic, $K := \lfloor \rho A \rfloor$. Having obtained some intuition about the system behavior, we will later look at the situation with a random number of nodes.

Suppose that the channel gains of sensors $h_i(t)$ are i.i.d. Rician distributed. Rician distribution is appropriate, especially when there is a line-of-sight between the sensors and the receiver, which is the case in SENMA. We use the notation $h_i = |\sqrt{\gamma/d^\alpha} + v|$, where $\sqrt{\gamma/d^\alpha}$ is a deterministic scalar ($\alpha \geq 2$ is the attenuation coefficient), v is complex Gaussian with zero mean and variance $\gamma/\kappa d^\alpha$ ($|\cdot|$ denotes the absolute value). The parameter $\kappa > 0$ is the ratio of the energy of the deterministic component to the energy of the random component.

A special case of the capacity expression (12) is when each h_i^2 is deterministic, and is equal to γ/d^α . Substituting h_i 's and K , we get

$$\begin{aligned} C &= \frac{1}{2} \log \left(1 + \frac{\gamma/d^\alpha K P}{\sigma^2} \right) \\ &= \frac{1}{2} \log \left(1 + \frac{\gamma/d^\alpha [\rho \pi^2 d^2 \tan^2 \theta] P}{\sigma^2} \right). \end{aligned} \quad (13)$$

⁴A more accurate model would have to account for relative positions of the nodes within the coverage area, e.g., path loss from the center is $1/d^\alpha$, but the path loss from the boundary of coverage is $1/(d/\cos \theta)^\alpha$ (α is the attenuation factor). However, this consideration makes the analysis intractable ($h_i(t)$, $i = 1, \dots$ would no longer be identically distributed), and obscures the basic tradeoffs we want to investigate. In general, one can obtain upper and lower bounds from the given rate expressions by assuming the sensors are always at the center or always at the boundary, respectively.

⁵This equation is the conditional mutual information, $(1/T) I(\mathbf{y}; \mathbf{x}_1, \dots, \mathbf{x}_N | h_1, \dots, h_N, \mathcal{J})$, where \mathbf{x}_i are i.i.d. $\mathcal{N}(0, P\mathbf{I})$.

When $\alpha \geq 2$, we see that the number of sensors in the coverage grows proportional to d^2 ; however, the signal strength attenuates with a faster rate $1/d^\alpha$. Therefore, the sum-rate is maximized when d is minimum and $K = 1$. In other words, to maximize the sum-rate, the mobile AP should *fly as low as possible* to boost the channel strength. Besides, the coverage area should be designed as small as possible, such that every time, the AP hears only from one sensor.

Next, we will look at the case with time-varying channels. The capacity upper bound

$$\begin{aligned} C &= \frac{1}{2} \mathbb{E}_{\mathbf{h}} \log \left(1 + \frac{PK \frac{1}{K} \sum_{i=1}^K h_i^2}{\sigma^2} \right) \\ &\leq \frac{1}{2} \log \left(1 + \frac{PK(\gamma/d^\alpha)(\kappa + 1)/\kappa}{\sigma^2} \right) := C' \end{aligned} \quad (14)$$

follows from Jensen's inequality [31]. This inequality is tight for large K , since when K is large, the random variable $(1/K) \sum_{i=1}^K h_i^2$ smooths out, and approaches its mean $(\gamma/d^\alpha)(\kappa + 1)/\kappa$. (Also $C' - C \rightarrow 0$ as $K \rightarrow \infty$, for a proof see [7]). From (14), we see that two main factors affect the sum-rate. First, having large K is good, since the random variable $(1/K) \sum_{i=1}^K h_i^2$ gets smoother, and C approaches its upper bound C' . However, having large K (keeping ρ constant) also means that d is large, and the signal strength γ/d^α attenuates too much. Tradeoff between these two factors yields that the optimal value of K , in general, is neither equal to one nor unbounded; it is somewhere in between. The numerical evaluation of C and C' confirms this intuition (Fig. 4(a), also see [32]). In numerical evaluation we have observed, however, that in several cases ($\alpha \geq 2.5$, or SNR is small, or κ is large) $K = 1$ is either optimal or very close to the optimal.

We are now in a position to relax the assumption that there are exactly K sensors in coverage. For simplicity, suppose that K is Poisson with mean $\mathbb{E}K = \rho A$. The numerical results are presented in Fig. 4(b) and [32]. The major difference between random and deterministic K is that when K is random, there is always a possibility of empty coverage. To avoid this situation, $\mathbb{E}K$ should not be chosen too small. However, as we have seen in the deterministic case, because of signal attenuation, $\mathbb{E}K$ should not be too large, either.

Notice that the capacity with random K , but fixed $h_i = h$, satisfies

$$C = \frac{1}{2} \mathbb{E}_K \log \left(1 + \frac{P \sum_{i=1}^K h^2}{\sigma^2} \right) \leq \frac{1}{2} \log \left(1 + \frac{Ph^2 \mathbb{E}K}{\sigma^2} \right) \quad (15)$$

from Jensen's inequality. A trajectory with fixed number of nodes within coverage ($\mathbb{E}K$) achieves this upper bound; such a trajectory is sum-rate-optimal if it exists. In general, the above bound indicates that the lower the variation in K , the higher the capacity.

So far we have analyzed the network capacity with constant sensor density. We will next consider the case where the flying altitude d is fixed, but ρ is varying. This scenario is important when the mobile AP can not get any closer to the ground than d meters due to the physical conditions. In such a case, one would consider increasing the sensor density to improve the network capacity (from (12), observe that C increases proportionally with K ; the greater the number of sensors, the higher the

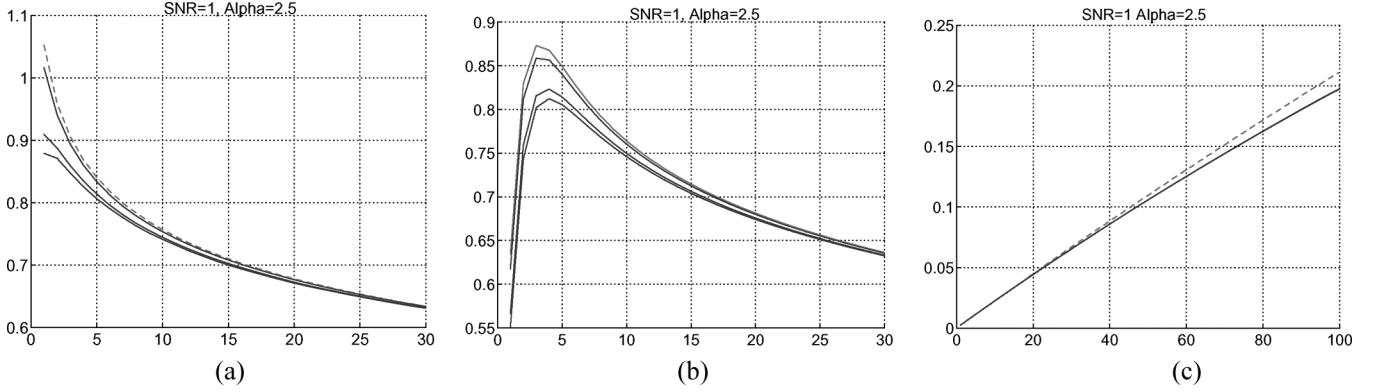


Fig. 4. (a) C (solid lines, $\kappa = 0.1, 1, 10$, bottom to top) and the upper bound C' (dashed line) in units of bits/channel use versus K . K determines the distance d via $K = \rho \pi^2 d^2 \tan^2 \theta$. The other parameters are $\gamma = 1$, $\rho = 1$ sensor/m², $\theta = 45^\circ$, $\text{SNR} := P(\kappa + 1)/(\kappa \sigma^2)$. (b) Number of sensors is Poisson distributed with the mean ρA . The y axis is the same as above, the x -axis shows ρA . (c) Same as (b), except that ρ is varying, $d = 10$ m is fixed. There are four curves in every figure, but several of them overlap and appear as one.

total transmission power, and therefore, the network capacity). For increasing ρ and fixed d (10 m), numerical evaluation of the capacity formula (12) is given in Fig. 4(c) and [32]. One normally would expect the capacity to be proportional to the logarithm of the average number of sensors (this follows from (12), where the term inside the logarithm is proportional to the number of sensors K). However, surprisingly, in Fig. 4, there is almost a linear correspondence between the network capacity and the network density. This is due to the fact that the sensor SNRs are small (this is the so-called *wideband regime* [33]), and the logarithm behaves like a linear function ($\log(1 + x) \approx x$ for small x). The conclusion is that increasing the network density is an effective way of improving the network capacity in low-power sensor networks.

C. SENMA With Multiple Noncooperative Mobile APs

In this section, we will first analyze the SENMA with two mobile APs, and then discuss generalizations to multiple APs. Let $J_1(t)$, $J_2(t)$ denote the location of two mobile APs in block t . Each mobile AP activates only its own coverage area. The received signal \mathbf{y}_i at AP $i = 1, 2$ is given by

$$\begin{aligned} \mathbf{y}_1 &= \sum_{i \in \mathcal{J}_1} h_i^1 \mathbf{x}_i + \lambda(J_1, J_2) \sum_{i \in \mathcal{J}_2 \setminus \mathcal{J}_1} h_i^1 \mathbf{x}_i + \mathbf{n}_1 \\ \mathbf{y}_2 &= \sum_{i \in \mathcal{J}_2} h_i^2 \mathbf{x}_i + \lambda(J_2, J_1) \sum_{i \in \mathcal{J}_1 \setminus \mathcal{J}_2} h_i^2 \mathbf{x}_i + \mathbf{n}_2 \end{aligned} \quad (16)$$

(the time index is suppressed for notational convenience). This notation is a natural extension of the one in previous subsection; $h_i^r \in \mathbb{R}$ is the channel gain from sensor i to the r th AP. As previously, we assume that the channel gains h_i^k are i.i.d. Rician in time and amongst users. The parameter $\lambda(J_k, J_r) \in \mathbb{R}$ is the attenuation of signal transmitted from the k th coverage area to the r th AP. $\lambda(\cdot)$ is assumed to be a function of distance between J_1 and J_2 , which is strictly decreasing with distance and upper bounded by 1.⁷ As a technical requirement, we suppose that the AP locations J_1, J_2 follow a stationary path (which can be periodic or random, according to an ergodic process).

When the APs do not have access to each other's received signals, we say that they do not cooperate. In this case, the

problem belongs to the class of *interference channels* whose capacity is yet unknown [34]. However, we know that certain rates are achievable when the sensors use Gaussian signaling, and the interference appears as Gaussian noise. Under this assumption, the interference comes to the denominator in the usual $\log(1 + \text{SNR})$ capacity expression, and the sum-rate

$$\begin{aligned} R_n &= \frac{1}{2} \mathbb{E}_{J_1, J_2} \mathbb{E}_{\mathbf{h}^1, \mathbf{h}^2} \\ &\times \left[\log \left(1 + \frac{P \sum_{i \in \mathcal{J}_1} (h_i^1)^2}{\sigma^2 + P \lambda^2(J_1, J_2) \sum_{i \in \mathcal{J}_2 \setminus \mathcal{J}_1} (h_i^1)^2} \right) \right. \\ &\left. + \log \left(1 + \frac{P \sum_{i \in \mathcal{J}_2} (h_i^2)^2}{\sigma^2 + P \lambda^2(J_2, J_1) \sum_{i \in \mathcal{J}_1 \setminus \mathcal{J}_2} (h_i^2)^2} \right) \right] \end{aligned} \quad (17)$$

is achievable; a rigorous proof follows from [7, Th. 1]. This is the summation of the rates achieved by the first and second APs. To achieve (17), the first AP needs to know instantaneous signal-to-interference-plus-noise ratios

$$\frac{P (h_i^1)^2}{\sigma^2 + P \lambda^2(J_1, J_2) \sum_{i \in \mathcal{J}_2 \setminus \mathcal{J}_1} (h_i^1)^2} \quad (18)$$

of sensors within its coverage, and similarly, so does the second AP.

To compute (17), one needs to take expectation with respect to the location of APs J_1, J_2 that are interpreted as random variables. Distribution of these two random variables is a design parameter, and its optimal value determines how the trajectory and relative positions of APs should be. To optimize the distribution of J_1, J_2 , observe the following upper bound on R_n :

$$\begin{aligned} R_n &\leq \frac{1}{2} \mathbb{E}_{J_1, J_2} \mathbb{E}_{\mathbf{h}^1, \mathbf{h}^2} \left[\log \left(1 + \frac{P \sum_{i \in \mathcal{J}_1} (h_i^1)^2}{\sigma^2} \right) \right. \\ &\left. + \log \left(1 + \frac{P \sum_{i \in \mathcal{J}_2} (h_i^2)^2}{\sigma^2} \right) \right]. \end{aligned} \quad (19)$$

This upper bound can be achieved arbitrarily closely if and only if $\lambda(J_1, J_2) \approx 0$ w.p. 1. This result says that to maximize the

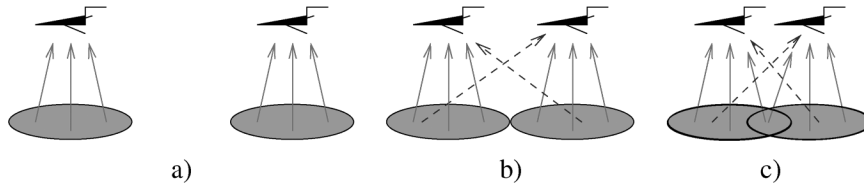


Fig. 5. Three possibilities for receiver cooperation. (a) Apart (no interaction). (b) Together (no overlap). (c) Overlap.

sum-rate in (17), the mobile APs should fly as separately as possible. In this way, the interference problem is avoided.⁶

We see that the upper bound in (19) is twice the capacity with single AP (12). Since the expressions are the same, the discussion about optimal choice of K and flying altitude in the previous section applies also to noninterfering multiple APs. When there are more than two APs, say, there are L of them, as long as the APs do not interfere with each other, the achievable rate is L times the capacity with single AP. When L is too large, interference between APs becomes unavoidable, and the sum-rate no longer increases linearly with L .

D. SENMA With Cooperative Mobile APs

In this section, we will examine the case where the mobile APs have access to each other's signals (i.e., the APs cooperate in reception). This is possible, for example, when the APs pass their received signal to a satellite, and the signals are decoded jointly at the satellite.

The system with cooperative APs can be viewed as a MAC channel with multiple receive antennas. A crucial parameter affecting the system performance is the coupling $\lambda(J_1, J_2)$ between these antennas, which is determined by the distance between APs. The main result of this section is that high coupling is desirable when the SNR is low, but zero coupling is the best at high SNR. This result, for example, implies that if the SNR is high, cooperation is not useful (the best rate with cooperation is same as the best noncooperative rate). However, at low SNR, cooperation can improve the achievable rate up to two times.

Another factor which affects the performance is the existence of overlap between coverage areas. APs getting too close to each other improves the coupling at the cost of reducing the total number of transmitting sensors [Fig. 5(c)]. The fewer number of transmitters, the lower the capacity, as it is the case with single AP. This is particularly a problem at low SNR, where

⁶Interestingly, the case without interference provides an upper bound not only on R_n , but also on the capacity of the interference channel [31]. Hence, the flying-apart strategy also maximizes the capacity of the interference channel.

⁷As in the single AP setup, (16) is simplistic, since the relative positions of the nodes within the coverage are not considered.

high coupling is desirable. We also investigate this tradeoff in the following.

Throughout this section, for simplicity, we assume that the number of sensors K within coverage is deterministic. We first focus on the case that the coverage areas are nonoverlapping. This means that the coupling varies between $\lambda = 0$ [Fig. 5(a)] and $\lambda = \lambda_0$, which denotes the highest λ without overlap [Fig. 5(b)]. We then consider the possibility of overlap, and find the optimal strategies at high and low SNR.

With cooperative APs, the system equation is same as the one in the noncooperative case. But unlike the noncooperative scenario, the information-theoretic limits with cooperating APs is well established (with cooperation, the system is a special case of the multiaccess channel). In case of no overlap, the sum-capacity is given by (20), shown at the bottom of the page, where $h_{i,j}^k$ is distributed i.i.d. with distribution the same as h_i^k (see Appendix A for a proof).

To analyze the system behavior, we first consider the case that the channel gains are constant $h := h_i^k$. Notice that the quantity in expectation in (20) depends on J_1, J_2 only through $\lambda(J_1, J_2)$. Therefore, we can express R_c as an expectation over λ , treating λ as a random variable. Substituting constant h , the R_c simplifies to

$$R_c = \mathbb{E}_\lambda \frac{1}{2} \left[\log(1 + \text{SNR}_T(1 - \lambda)^2) + \log(1 + \text{SNR}_T(1 + \lambda)^2) \right] \quad (21)$$

where $\text{SNR}_T := h^2 K P / \sigma^2$ (total SNR).

Next, we will maximize

$$r(\lambda) := \frac{1}{2} \left[\log(1 + \text{SNR}_T(1 - \lambda)^2) + \log(1 + \text{SNR}_T(1 + \lambda)^2) \right]$$

in (21) with respect to $0 \leq \lambda \leq \lambda_0$. The maximum provides an upper bound to R_c . Furthermore, the maximizing λ can be converted to the optimal distance between APs, and enables us to determine the optimal strategy with multiple APs.

Lemma 1: The $r(\lambda)$ attains its maximum at $\lambda = \lambda_0$ if

$$\text{SNR}_T \leq \frac{2}{2 - \lambda_0^2} \quad (22)$$

and at $\lambda = 0$ otherwise.

$$R_c = \frac{1}{2} \mathbb{E}_{J_1, J_2} \mathbb{E}_{h^1, h^2} \log \left\{ \left[1 + \frac{P}{\sigma^2} \left[\sum_{i=1}^K (h_{i,1}^1)^2 + \lambda^2(J_2, J_1) (h_{i,2}^1)^2 \right] \right] \cdot \left[1 + \frac{P}{\sigma^2} \left[\sum_{i=1}^K (h_{i,2}^2)^2 + \lambda^2(J_1, J_2) (h_{i,1}^2)^2 \right] \right] - \frac{P^2}{\sigma^4} \lambda^4(J_1, J_2) \left[\sum_{i=1}^K h_{i,1}^1 h_{i,1}^2 + h_{i,2}^1 h_{i,2}^2 \right]^2 \right\} \quad (20)$$

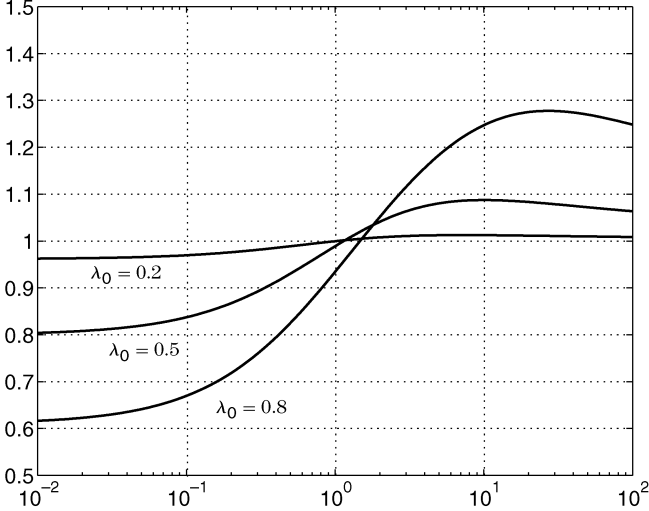


Fig. 6. $r(0)/r(\lambda_0)$ versus SNR_T .

Note that the lemma implies that if SNR_T is above the critical threshold (22), cooperation does not help, i.e., the optimal λ is zero, and the best cooperative rate is same as the noncooperative rate. The lemma also implies that $r(\lambda)$ happens to be maximum either at $r(\lambda_0)$ or at $r(0)$, which correspond to two different strategies; flying in formation in the former case, and to fly apart in the latter case. To obtain a better idea about the relative performance of these strategies, the ratio $r(0)/r(\lambda_0)$ is plotted in Fig. 6.

Some numerical results about the sum-rate with time-varying Rician channels are given in Fig. 7. This case is harder to analyze, and we resort to the numerical evaluations. As in the deterministic case, we define $r(\lambda_0)$ as the rate achieved when the APs are neighboring [$\lambda(J_1, J_2) = \lambda_0$ w.p. 1 in (20)], and $r(0)$ as the rate achieved when the APs are always apart ($\lambda(J_1, J_2) = 0$). From Fig. 7, we see that the intuition from the deterministic channels largely carries over to the random channels (i.e., flying in formation is better when SNR is low; otherwise, flying apart is better). However, the gain of flying together, compared with flying apart, significantly varies depending on the network parameters.

Next, we will consider overlap in coverage areas. For simplicity, assume that the channel gains h are constant. We use $\beta \in \{0, (1/K), (2/K), \dots, 1\}$ to denote the fraction of sensors covered *only* by a single AP (i.e., each AP has βK sensors only in its own coverage, and $(1-\beta)K$ sensors covered by both APs). We view β as function of λ (λ determines the distance between APs, and the distance determines β). The cooperative rate, allowing overlap, is given by

$$R_c = \mathbb{E}_\lambda \frac{1}{2} \left[\log(1 + \beta \text{SNR}_T (1 - \lambda)^2) + \log(1 + 2(1 - \beta) \text{SNR}_T + \beta \text{SNR}_T (1 + \lambda)^2) \right] \quad (23)$$

(see Appendix B for a proof). As before, define $r(\lambda)$ as the function inside the expectation.

At low SNR_T , we have the approximation

$$\begin{aligned} r(\lambda) &\approx \frac{1}{2} \left[\beta \text{SNR}_T (1 - \lambda)^2 + 2(1 - \beta) \text{SNR}_T \right. \\ &\quad \left. + \beta \text{SNR}_T (1 + \lambda)^2 \right] \\ &= \text{SNR}_T (1 + \beta \lambda^2). \end{aligned} \quad (24)$$

More precisely, we have $r(\lambda)/\text{SNR}_T(1 + \beta \lambda^2) \rightarrow 0$ as $\text{SNR}_T \rightarrow 0$. (This comes from the Taylor series expansion of $\log(1 + x) = x + O(x^2)$ for $|x| < 1$.) So at low SNR, the optimal coupling (and, coverage) is the one that maximizes $\beta \lambda^2$; the optimal strategy is either flying together (no overlap) or partial overlap. Full overlap is never optimal since it corresponds to $\beta = 0$.

At high SNR

$$\begin{aligned} r(\lambda) &\approx \frac{1}{2} \left[\log(\beta \text{SNR}_T (1 - \lambda^2)) \right. \\ &\quad \left. + \log(2(1 - \beta) \text{SNR}_T + \beta \text{SNR}_T (1 + \lambda)^2) \right] \\ &= \frac{1}{2} \log \left[\text{SNR}_T^2 (1 - \lambda^2) (2\beta(1 - \beta) + \beta^2 (1 + \lambda)^2) \right] \\ &= \frac{1}{2} \log \left[\text{SNR}_T^2 (1 - \lambda^2) (2\beta + \beta^2 [(1 + \lambda)^2 - 2]) \right]. \end{aligned} \quad (25)$$

We need to maximize the last expression with respect to λ and β (which is a function of λ). Instead of this doing this, we consider an upper bound by maximizing over a rectangular domain $0 \leq \beta \leq 1, 0 \leq \lambda \leq 1$ where β and λ are not coupled. Fix $\lambda \leq 1, 0 \leq \beta \leq 1$. This is a quadratic, which is concave \cap . Hence, it is increasing from $\beta = -\infty$ to the point where its derivative is zero, i.e.,

$$2 + 2\beta [(1 + \lambda)^2 - 2] = 0 \Rightarrow \beta = \frac{1}{2 - (1 + \lambda)^2}.$$

This β exceeds 1. Therefore, the quadratic is maximized at $\beta = 1$. Substituting $\beta = 1$ and continuing from (25)

$$\begin{aligned} &\leq \max_{0 \leq \lambda \leq 1} \frac{1}{2} \log \{ \text{SNR}_T^2 (1 - \lambda^2)^2 \} \\ &\leq \frac{1}{2} \log \{ \text{SNR}_T^2 \} \\ &\leq \frac{1}{2} \log(1 + \text{SNR}_T)^2. \end{aligned} \quad (26)$$

The last rate is the one achieved when flying apart. Inequality (26) becomes equality only if $\lambda = 0$. Hence, we see that the flying-apart strategy is the best at high SNR.

E. A General Approach to SENMA With Multiple Cooperative APs

In this section, we generalize the analysis done for two mobile APs to arbitrary number of APs. We provide general formulas for the sum-capacity with arbitrary number of APs, and show that the optimal strategy is same as that with two APs: if the total SNR is low, then the APs should fly in formation. At high SNR, however, it is best to place APs as far apart as possible.

Consider the scenario that there exists L mobile APs, each with K sensors in their coverage. First, assume that the coverage areas of APs are disjoint, and the signal strength from the i th coverage area to j th APs is attenuated by $\lambda(J_i, J_j)$. Then, the sum-capacity is given by

$$R_c = \frac{1}{2} \mathbb{E}_{J_1, \dots, J_L} \mathbb{E}_{\mathbf{h}^1, \dots, \mathbf{h}^L} \log \det \left[\mathbf{I} + \frac{P}{\sigma^2} \mathbf{A} \mathbf{A}^t \right] \quad (27)$$

where the entries of matrix $\mathbf{A} \mathbf{A}^t$ are given by

$$\mathbf{A} \mathbf{A}^t = \left[(\mathbf{A} \mathbf{A}^t)_{n,m} = \sum_{l=1}^L \sum_{i=1}^K \lambda(J_l, J_n) \lambda(J_l, J_m) h_{i,l}^n h_{i,l}^m \right]$$

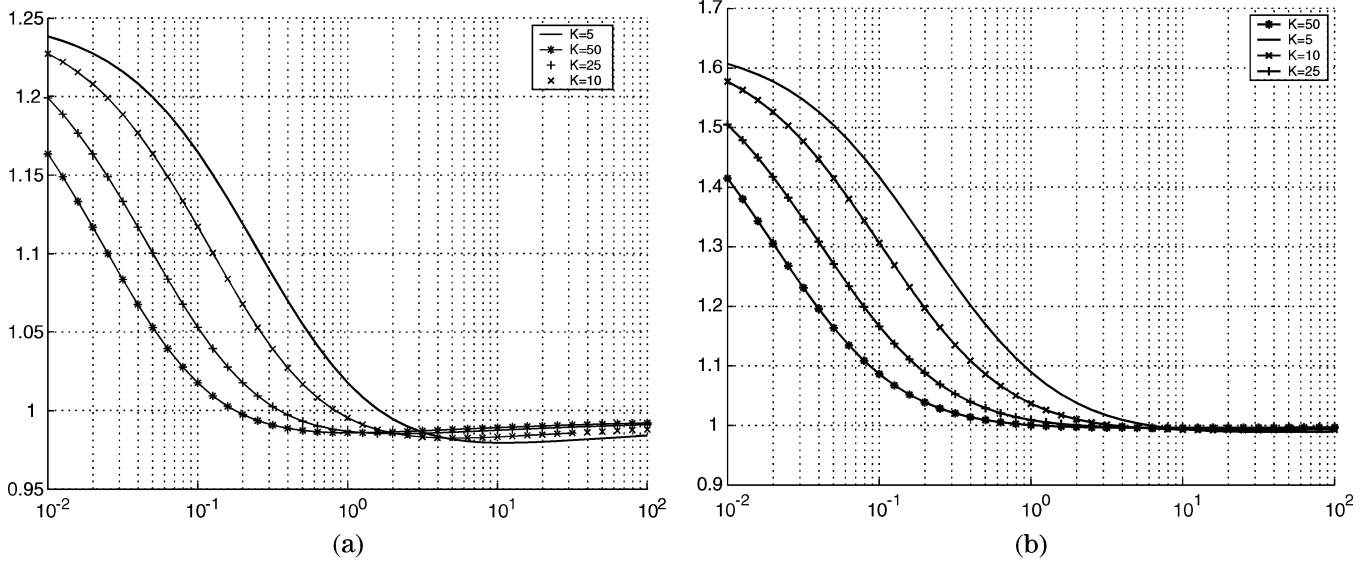


Fig. 7. $r(\lambda_0)/r(0)$ versus $\text{SNR} = \mathbb{E}(h_i^2)P/\sigma^2$ ($\kappa = 1$). (a) $\lambda_0 = 0.5$. (b) $\lambda_0 = 0.8$.

(can be obtained as a direct extension of the argument in Appendix A).

The sum-capacity expression can be better understood in case of deterministic channel gains ($h_{i,j}^k = h$)

$$R_c = \frac{1}{2} \mathbb{E}_{J_1, \dots, J_L} \log \det[\mathbf{I} + \text{SNR}_T \mathbf{A} \mathbf{A}^t] \quad (28)$$

where SNR_T is defined as before, and $(\mathbf{A} \mathbf{A}^t)_{n,m} = \sum_{l=1}^L \lambda(J_l, J_n) \lambda(J_l, J_m)$.

We make these natural assumptions for the following lemma: $\lambda(J_i, J_i) = 1$, $0 \leq \lambda(J_i, J_j) \leq 1$, and $\lambda(J_i, J_j) = \lambda(J_j, J_i) \forall i, j$.

Lemma 2: Consider a network with L mobile APs with nonoverlapping coverage areas.

- 1) At high SNR ($\text{SNR}_T \rightarrow \infty$), the optimal strategy is to let mobile APs fly as far apart as possible, i.e., $\lambda(J_i, J_j) = 0 \forall i \neq j$.
- 2) At low SNR ($\text{SNR}_T \rightarrow 0$) the optimal strategy is the one that maximizes $\sum_{i,j=1}^L \lambda^2(J_i, J_j)$ with respect to J_1, \dots, J_L . This corresponds to mobile APs flying as close as possible.

Proof: We need to maximize $\log \det[\mathbf{I} + \text{SNR}_T \mathbf{A} \mathbf{A}^t]$ with respect to J_1, \dots, J_L . As $\text{SNR}_T \rightarrow \infty$, we have the asymptotic expression

$$\log \det[\mathbf{I} + \text{SNR}_T \mathbf{A} \mathbf{A}^t] \approx \log(\text{SNR}_T) + 2 \log |\det \mathbf{A}|. \quad (29)$$

Since the matrix \mathbf{A} is symmetric and each of its entries are in $[0, 1]$, we can use the Hadamard inequality [31] to get $2 \log |\det \mathbf{A}| \leq 2 \log \prod_{i=1}^L \mathbf{A}_{ii}$, with equality if and only if $\mathbf{A}_{ij} = 0 \forall i \neq j$. This exactly gives the condition for optimality at high SNR.

As $\text{SNR}_T \rightarrow 0$, we have the Taylor series expansion

$$\log \det[\mathbf{I} + \text{SNR}_T \mathbf{A} \mathbf{A}^t] \approx \text{SNR}_T \text{tr}(\mathbf{A} \mathbf{A}^t) \quad (30)$$

where $\text{tr}(\cdot)$ denotes the trace of a matrix. Hence, the optimal strategy at low SNR should maximize $\text{tr}(\mathbf{A} \mathbf{A}^t) = \sum_{i,j=1}^L \lambda^2(J_i, J_j)$. For the λ 's to be large, the APs need to be as close as possible. ■

Lemma 2 addresses APs without overlapping coverage areas. We will consider overlapping coverages next. To this end, let $\beta_{\mathcal{S}}, \mathcal{S} \subset \{1, \dots, K\}$ denote the fraction of nodes that are in the joint coverage of the APs in \mathcal{S} . Notice that there are $2^K - 1$ such possible regions for nodes, $0 \leq \beta_{\mathcal{S}} \leq 1$ and $\sum_{\mathcal{S}: i \in \mathcal{S}} \beta_{\mathcal{S}} = 1$ for each i . In short, the $\beta_{\mathcal{S}}$ notation generalizes the β notation in the previous section to multiple APs. As before, $\beta_{\mathcal{S}}$ is a function of the AP locations J_1, \dots, J_L , but we will not write this dependency explicitly to simplify the notation. Another notation we need to generalize is $\lambda(\mathcal{S}, J_i)$, which is the attenuation of channel gains from the joint coverage of $\mathcal{S} \subset \{1, \dots, K\}$ to the i th AP.

In case of identical channel gains, the sum-rate of the SENMA with overlapping coverage areas is given by

$$R_c = \frac{1}{2} \mathbb{E}_{J_1, \dots, J_L} \log \det[\mathbf{I} + \text{SNR}_T \mathbf{A} \mathbf{A}^t] \quad (31)$$

where the matrix is now given by $(\mathbf{A} \mathbf{A}^t)_{n,m} = \sum_{\mathcal{S} \subset \{1, \dots, L\}} \beta_{\mathcal{S}} \lambda(\mathcal{S}, J_n) \lambda(\mathcal{S}, J_m)$ (see Appendix C for the proof). The following lemma generalizes **Lemma 2**.

Lemma 3: In a network with L mobile APs with overlapping coverage areas, the strategy that maximizes $\det |\mathbf{A} \mathbf{A}^t|$ and $\sum_{i=1}^L \sum_{\mathcal{S} \subset \{1, \dots, L\}} \beta_{\mathcal{S}} \lambda^2(\mathcal{S}, J_i)$ with respect to J_1, \dots, J_L maximizes the sum-capacity at high and low SNRs, respectively.

Proof: Follows from (29) and (30). ■

At low SNR, an interpretation of the capacity-maximizing strategy is that the mobile APs should fly close enough to maximize λ 's, however should fly apart enough so that a large area is covered. Where the optimal point lies is dependent on the number of APs and the explicit structure of λ s.

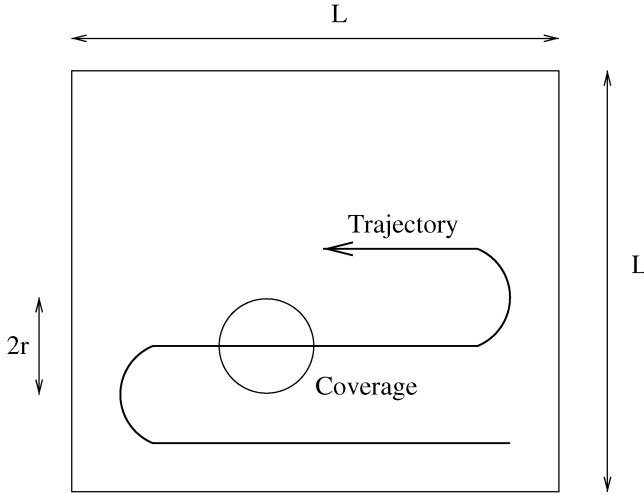


Fig. 8. Trajectory of mobile AP.

IV. CAPACITY VERSUS DELAY AND TOTAL DATA-COLLECTION TIME

Delay and total data-collection time are other important metrics besides capacity. These metrics are inversely proportional with each other, because if the mobile APs take longer to traverse the network and collect all data, then sensors have to wait longer before each AP visit.

Total data-collection time has a curious relationship with the coverage area of APs. In Section III, we argued that smaller coverage, which means lower flying altitude, generally increases the capacity. Smaller coverage, on the other hand, also increases the data-collection time, because the mobile takes longer to traverse the network. The relationship between coverage area and the travel time in a two-dimensional network are exemplified in Fig. 8. Here, it is obvious that the travel time at constant speed is proportional to $L^2/(2r)$ (travel time along the x-axis is about L/v , where v is the velocity. The mobile has to scan the area $L/(2r)$ times horizontally).

Larger coverage, however, does not always mean reduced travel time. If the mobile travels at higher altitude, then the capacity is also decreased, implying that the mobiles have to roam slower to collect all data. Here, we are seeing two ends of an interesting tradeoff: 1) in the “mobile-speed-limited” regime, there is abundant capacity, although the travel time is large; 2) in the “capacity-limited” regime, the mobile could traverse the network faster, but data throughput limitations do not allow that. In practice, the mobile altitude should be chosen such that the network has abundant capacity to allow fast data transfer, but also the mobile APs also have sufficient coverage to travel the network faster.

V. CONCLUSION

We considered the SENMA architecture for sensor networks. We first analyzed its energy consumption, and compared it with that of the multihop ad hoc architecture. We argued that SENMA achieves significant energy savings by shifting the responsibility of routing and network control from sensors to the mobile APs. We then considered the design of network parameters such as mobile AP’s flying altitude, trajectory, and coverage. We also investigated the case with multiple APs both for noncooperative and cooperative receptions.

One may question whether it is realistic to rely on low-power sensors to reach mobile APs far away. This concern is mild for APs which are low-altitude aerial or ground-based. For general mobile APs, schemes have been developed in [4], [6], and [9] that allow transmission to distances that normally would not be reachable. The key is to trade the size of the network for power efficiency by exploiting multiuser diversity via opportunistic transmissions, an idea that has been proposed in an information-theoretic setting [35], [36].

SENMA is most relevant to applications where a large number of inexpensive and low-power sensors are deployed, and the data is low-rate and *delay-tolerant*. This architecture is, perhaps, less applicable for extremely delay-sensitive applications. In such applications, the trajectory of mobile AP may need to be controlled, depending on field readings and delay requirements. Algorithms for such control and analysis of tracking performance constitute an interesting area for future work.

APPENDIX

A. Achievable Rate With Cooperation

Recall the assumptions that the coverage areas do not overlap, and each coverage area has K users. These enable us to rewrite (20) as

$$\begin{aligned} y_1 &= \sum_{i=1}^K h_{i,1}^1 x_{i,1} + \lambda(J_1, J_2) \sum_{i=1}^K h_{i,2}^1 x_{i,2} + n_1 \\ y_2 &= \sum_{i=1}^K h_{i,2}^2 x_{i,2} + \lambda(J_2, J_1) \sum_{i=1}^K h_{i,1}^2 x_{i,1} + n_2 \end{aligned} \quad (32)$$

where we use a second subscript in h and x to refer to the coverage area from which the signal is coming, i.e., $x_{i,j}$ refers to the symbol of the i th sensor in the j th coverage area, and $h_{i,j}^k$ is its channel gain to the k th AP. Following arguments in [8], it is easy to see that Gaussian codebooks achieve the capacity, and the maximum sum-rate is given by $I(\{x_{i,j}\}; y_1, y_2 | \{h_{i,j}^k\}, J_1, J_2)$ where x_i are i.i.d. $\mathcal{N}(0, P)$. Equation (32) can be viewed as a multiple-input multiple-output system with the transfer matrix shown in the equation at the bottom of the page. A well-known formula for $I(\{x_{i,j}\}; y_1, y_2)$ for fixed $\{h_{i,j}^k\}, J_1, J_2$ is given by $(1/2) \log \det(\mathbf{I} + (P/\sigma^2) \mathbf{A} \mathbf{A}^t)$ (see, e.g., [37]), where we have

$$\mathbf{A} := \begin{bmatrix} h_{1,1}^1 & \cdots & h_{K,1}^1 & \lambda(J_1, J_2) h_{1,2}^1 & \cdots & \lambda(J_1, J_2) h_{K,2}^1 \\ \lambda(J_1, J_2) h_{1,1}^2 & \cdots & \lambda(J_1, J_2) h_{K,1}^2 & h_{1,2}^2 & \cdots & h_{K,2}^2 \end{bmatrix}$$

$$\mathbf{A}\mathbf{A}^t = \begin{bmatrix} \sum_{i=1}^K \left[(h_{i,1}^1)^2 + \lambda^2(J_2, J_1) (h_{i,2}^1)^2 \right] & \lambda^2(J_2, J_1) \sum_{i=1}^K [h_{i,1}^1 h_{i,1}^2 + h_{i,2}^1 h_{i,2}^2] \\ \lambda^2(J_2, J_1) \sum_{i=1}^K [h_{i,1}^1 h_{i,1}^2 + h_{i,2}^1 h_{i,2}^2] & \sum_{i=1}^K \left[(h_{i,2}^2)^2 + \lambda^2(J_1, J_2) (h_{i,1}^2)^2 \right] \end{bmatrix}$$

$$\mathbf{A} := \begin{bmatrix} h_{1,1}^1 & \cdots & h_{\beta K,1}^1 & h_{\beta K+1,1}^1 & \cdots & h_{K,1}^1 & \lambda h_{1,2}^1 & \cdots & \lambda h_{\beta K,2}^1 \\ \lambda h_{1,1}^2 & \cdots & \lambda h_{\beta K,1}^2 & h_{\beta K+1,1}^2 & \cdots & h_{K,1}^2 & h_{1,2}^2 & \cdots & h_{K,2}^2 \end{bmatrix} \quad (33)$$

the result found in the equation at the top of the page. We get (20) by averaging the log det expression over $\{h_{i,j}^k\}, J_1, J_2$.

B. Proof of Equation (23)

The cooperative system with overlap can be represented by a transfer matrix, as in the nonoverlap case shown in (33) at the top of the page ($\lambda(J_1, J_2)$ is abbreviated as λ for compactness). This matrix is such that the first βK columns are channel gains from sensors only in the first AP's coverage, the middle $(1 - \beta)K$ columns are sensors in both coverages, and the last βK is only in the second AP's coverage. After some algebra, expectation of $(1/2) \log \det(\mathbf{I} + (P/\sigma^2)\mathbf{A}\mathbf{A}^t)$ gives (23).

C. Proof of Equation (31)

Equation (31) is obtained in the same way as (23) is obtained, shown in Appendix B. The main difference in the case of L mobile APs is that there exist $2^L - 1$ blocks in the matrix \mathbf{A} defined in (33). There exist $2^2 - 1 = 3$ blocks in (33), since there are only two APs. Writing the analogous equation for (33) immediately gives (31).

D. Proof of Lemma 1

The function $r(\lambda)$ is twice differentiable, therefore, its maximum occurs either at $r'(\lambda) = 0$ or at the boundaries of the domain $0 \leq \lambda \leq \lambda_0$. Observe that

$$r'(\lambda) = \frac{\text{SNR}_T(\lambda - 1)}{1 + \text{SNR}_T(\lambda - 1)^2} + \frac{\text{SNR}_T(\lambda + 1)}{1 + \text{SNR}_T(\lambda + 1)^2}.$$

Therefore, $r'(\lambda) = 0$ if and only if

$$\begin{aligned} (\lambda - 1)(1 + \text{SNR}_T(\lambda + 1)^2) + (\lambda + 1)(1 + \text{SNR}_T(\lambda - 1)^2) \\ = 2\lambda [1 + \text{SNR}_T(\lambda^2 - 1)] \end{aligned} \quad (34)$$

is zero. The only positive root of this equation is $\lambda = \sqrt{1 - 1/\text{SNR}_T}$, which is real only for $\text{SNR}_T \geq 1$. Assuming that this is the case, compute

$$r\left(\sqrt{\frac{\text{SNR}_T - 1}{\text{SNR}_T}}\right) = \frac{1}{2} \log(4\text{SNR}_T). \quad (35)$$

Observe that this number is $\leq r(0) = (1/2) \log(1 + \text{SNR}_T)^2$. Therefore, the possibilities for the extremum reduce to $\lambda = 0$ and $\lambda = \lambda_0$. The rest is straightforward algebra to show that

$$r(0) \leq r(\lambda_0) \Leftrightarrow \text{SNR}_T \leq \frac{2}{2 - \lambda_0^2}.$$

REFERENCES

- [1] L. Tong, Q. Zhao, and S. Adireddy, "Sensor networks with mobile agents," in *Proc. Int. Symp. Mil. Commun.*, Boston, MA, Oct. 2003, vol. 1, pp. 688–693.
- [2] K. Sohrabi, B. Manriquez, and G. Pottie, "Near ground wideband channel measurement," in *Proc. 49th Veh. Technol. Conf.*, Houston, TX, May 1999, pp. 571–574.
- [3] G. Pottie and W. Kaiser, "Wireless integrated network sensors," *Commun. ACM*, vol. 43, pp. 51–58, May 2000.
- [4] P. Venkatasubramanian, S. Adireddy, and L. Tong, "Sensor networks with mobile agents: Optimal random access and coding," *IEEE J. Sel. Areas in Commun.: Special Issue Sensor Netw.*, vol. 22, no. 6, pp. 1058–1068, Aug. 2004.
- [5] Q. Zhao and L. Tong, "Distributed opportunistic transmission for wireless sensor networks," in *Proc. ICASSP*, May 2004, vol. 3, pp. 833–836.
- [6] —, "QoS specific information retrieval for densely deployed sensor network," in *Proc. Mil. Commun. Conf.*, Boston, MA, Oct. 2003, vol. 1, pp. 591–596.
- [7] S. Shamai (Shitz) and A. D. Wyner, "Information-theoretic considerations for symmetric cellular, multiple-access fading channels—Part I," *IEEE Trans. Inf. Theory*, vol. 43, no. 6, pp. 1877–1894, Nov. 1997.
- [8] —, "Information-theoretic considerations for symmetric cellular, multiple-access fading channels—Part II," *IEEE Trans. Inf. Theory*, vol. 43, no. 6, pp. 1895–1911, Nov. 1997.
- [9] P. Venkatasubramanian, S. Adireddy, and L. Tong, "Opportunistic ALOHA and cross layer design for sensor networks," in *Proc. Mil. Commun. Conf.*, Boston, MA, Oct. 2003, vol. 1, pp. 705–710.
- [10] P. Venkatasubramanian, Q. Zhao, and L. Tong, "Sensor networks with multiple mobile access points," in *Proc. Conf. Inf. Sci. Syst.*, Princeton, NJ, March 2004, CD-ROM.
- [11] J. Akyildiz, W. Su, Y. Sankarasubramanian, and E. Cayirci, "A survey on sensor networks," *IEEE Commun. Mag.*, vol. 40, no. 8, pp. 102–114, Aug. 2002.
- [12] K. Sohrabi, J. Gao, V. Ailawadhi, and G. Pottie, "Protocols for self-organization of a wireless sensor network," *IEEE Pers. Commun. Mag.*, pp. 16–27, Oct. 2000.
- [13] W. Zhao and M. Ammar, "Message ferrying: Proactive routing in highly-partitioned wireless ad hoc networks," in *Proc. IEEE Workshop Future Trends Distrib. Comput. Syst.*, Puerto Rico, May 2003, p. 308.
- [14] N. Bansal and Z. Liu, "Capacity, delay and mobility in wireless ad-hoc networks," in *Proc. INFOCOM*, San Francisco, CA, Mar. 30–Apr. 3 2003, vol. 2, pp. 1553–1563.
- [15] C. Cunningham and R. Roberts, "An adaptive path planning algorithm for cooperating unmanned air vehicles," in *Proc. IEEE Int. Conf. Robot. Autom.*, 2001, vol. 4, pp. 3981–3986.
- [16] T. Furukawa, F. Bourgault, H. Durrant-Whyte, and G. Dissanayake, "Dynamic allocation and control of coordinated UAVs to engage multiple targets in a time-optimal manner," in *Proc. IEEE Int. Conf. Robot. Autom.*, New Orleans, LA, Apr. 26–May 1 2004, pp. 2353–2358.
- [17] J. Sutcliffe, P. Riseborough, and H. Durrant-Whyte, "Decentralised data fusion applied to a network of unmanned aerial vehicles," in *Proc. Inf., Decision, Control Conf.*, 2002, pp. 71–76.
- [18] J. Gao, "Analysis of energy consumption for ad hoc wireless sensor networks using a bit-meter-per-Joule metric IPN Prog. Rep. 42-150, Aug. 2002 [Online]. Available: (http://ipnpr.jpl.nasa.gov/progress_report/42-150/150L.pdf)
- [19] M. Bhardwaj, T. Garnett, and A. Chandrakasan, "Upper bounds on the lifetime of sensor networks," in *Proc. IEEE Int. Conf. Commun.*, 2001, pp. 785–790.
- [20] E. Duarte-Melo and M. Liu, "Energy efficiency of many-to-one communications in wireless networks," in *Proc. IEEE 45th Midwest Symp. Circuits Syst.*, Tulsa, OK, 2002, vol. 1, pp. 615–618.

- [21] E. Shih, S. Cho, N. Ickes, R. Min, A. Sinha, A. Wang, and A. Chandrakasan, "Physical layer driven protocol and algorithm design for energy-efficient wireless sensor networks," in *Proc. ACM MOBICOM*, Rome, Italy, Jul. 2001, pp. 272–286.
- [22] J. Barros and S. D. Servetto, "On the capacity of the reachback channel in wireless sensor networks," in *Proc. IEEE Workshop Multimedia Signal Process.*, U.S. Virgin Islands, Dec. 2002, pp. 408–411.
- [23] J. Barros and S. D. Servetto, *Coding Theorems for the Sensor Reachback Problem With Partially Cooperating Nodes*, ser. Discr. Math. Theoret. Comput. Sci. (DIMACS) Ser. on Netw. Inf. Theory. Providence, RI: Amer. Math. Soc. (AMS), 2003.
- [24] W. Heinzelman, A. Chandrakasan, and H. Balakrishnan, "Energy-efficient communication protocols for wireless microsensor networks," in *Proc. Hawaiian Int. Conf. Syst. Sci.*, Maui, HI, Jan. 2000, vol. 2, pp. 1–10.
- [25] P. Gupta and P. R. Kumar, "The capacity of wireless networks," *IEEE Trans. Inf. Theory*, vol. 46, no. 2, pp. 388–404, Mar. 2000.
- [26] Q. Zhao and L. Tong, "Energy efficiency of large-scale wireless networks: Proactive vs. reactive networking," *IEEE J. Sel. Areas Commun., Special Issue Adv. Mil. Wireless Commun.*, vol. 23, no. 5, pp. 1100–1112, May 2005.
- [27] R. Min and A. Chandrakasan, "Energy-efficient communication for ad-hoc wireless sensor networks," in *Proc. 35th Asilomar Conf. Signals, Syst., Comput.*, Nov. 2001, vol. 1, pp. 139–143.
- [28] M. Haenggi, "The impact of power amplifier characteristics on routing in random wireless networks," in *Proc. IEEE Global Commun. Conf.*, 2003, vol. 1, pp. 513–517.
- [29] —, "Twelve reasons not to route over many short hops," in *Proc. IEEE Veh. Technol. Conf.*, 2004, vol. 5, pp. 3130–3134.
- [30] —, "Routing in ad hoc networks—A wireless perspective," in *Proc. 1st Int. Conf. Broadband Netw.*, 2004, pp. 652–660.
- [31] T. Cover and J. Thomas, *Elements of Information Theory*. New York: Wiley, 1991.
- [32] G. Mergen, Q. Zhao, and L. Tong, Capacity figures for SENMA [Online]. Available: http://acsp.ece.cornell.edu/papers/tcom_addition.pdf
- [33] S. Verdú, "Spectral efficiency in the wideband regime," *IEEE Trans. Inf. Theory*, vol. 48, no. 6, pp. 1319–1343, Jun. 2002.
- [34] E. C. van der Meulen, "Some reflections on the interference channel," in *Communications and Cryptography: Two Sides of One Tapestry*, R. E. Blahut, Ed. et al. Boston, MA: Kluwer, 1994.
- [35] R. Knopp and P. A. Humblet, "Information capacity and power control in single cell multi-user communications," in *Proc. Int. Conf. Commun.*, Seattle, WA, Jun. 1995, pp. 331–335.
- [36] P. Viswanath, D. N. C. Tse, and R. Laroia, "Opportunistic beamforming using dumb antennas," *IEEE Trans. Inf. Theory*, vol. 48, no. 6, pp. 1277–1294, Jun. 2002.
- [37] I. E. Telatar, "Capacity of multi-antenna Gaussian channels," *Eur. Trans. Telecommun.*, vol. 10, no. 6, pp. 585–595, Nov.–Dec. 1999.



Gökhan Mergen (S'99–M'06) was born in Ankara, Turkey, in 1978. He received the B.S. degree in electrical and electronics engineering and in mathematics from Middle East Technical University (METU), Ankara, Turkey, in 2000. He received the M.S. and Ph.D. degrees in electrical and computer engineering from Cornell University, Ithaca, NY, in 2005.

His industry experience includes work at Bell Labs, Lucent Technologies, during summer 2003. He is currently with Qualcomm, Campbell, CA. His

research interests lie in the areas of communications theory, information theory, data networks, and statistical signal processing.



Qing Zhao (S'97–M'02) received the B.S. degree from Sichuan University, Chengdu, China, in 1994, the M.S. degree from Fudan University, Shanghai, China, in 1997, and the Ph.D. degree from Cornell University, Ithaca, NY, in 2001, all in electrical engineering.

From 2001 to 2003, she was a Communication System Engineer with Aware, Inc., Bedford, MA. She returned to academe in 2003 as a Postdoctoral Research Associate with the School of Electrical and Computer Engineering, Cornell University. In 2004,

she joined the Department of Electrical and Computer Engineering, University of California, Davis, where she is currently an Assistant Professor. Her research interests are in the general area of signal processing, communication systems, wireless networking, and information theory. Specific topics include adaptive signal processing for communications, design and analysis of wireless and mobile networks, fundamental limits on the performance of large scale ad hoc and sensor networks, and energy-constrained signal processing and networking techniques.

Dr. Zhao received the IEEE Signal Processing Society Young Author Best Paper Award.



Lang Tong (S'87–M'91–SM'01–F'05) received the B.E. degree from Tsinghua University, Beijing, China, and the M.S. and Ph.D. degrees from the University of Notre Dame, Notre Dame, IN.

He is a Professor in the School of Electrical and Computer Engineering, Cornell University, Ithaca, NY. He was a Postdoctoral Research Affiliate at the Information Systems Laboratory, Stanford University, Stanford, CA. Prior to joining Cornell University, he was on the faculty at the University of Connecticut and West Virginia University. He

was also the 2001 Cor Wit Visiting Professor at the Delft University of Technology, Delft, The Netherlands. His areas of interest include statistical signal processing, wireless communications, communication networks and sensor networks, and information theory.

Dr. Tong received the Young Investigator Award from the Office of Naval Research in 1996, the Outstanding Young Author Award from the IEEE Circuits and Systems Society in 1994, the 2004 Best Paper Award from the IEEE Signal Processing Society, and the 2004 Leonard G. Abraham Prize from the IEEE Communications Society.